Supplementary Material: Two-dimensional Fresnel reflection-based columnar photonic scintillator

Tatsunori Shibuya[1,2*], Eichi Terasawa[1,2*], Hiromi Kimura[1,2], and Takeshi Fujiwara[1,2*]

E-mail: t-shibuya@aist.go.jp, wisdom.terasawa@aist.go.jp, fujiwara-t@aist.go.jp

[1] Non-Destructive Imaging Research Team, Integrated Research Center for Resilient Infrastructure, National Institute of Advanced Industrial Science and Technology (AIST), 1-1-1 Umezono, Tsukuba 305-8568, Japan.

[2] Research Institute for Measurement and Analytical Instrumentation (RIMA), National Metrology Institute of Japan (NMIJ), National Institute of Advanced Industrial Science and Technology (AIST), 1-1-1 Umezono, Tsukuba 305-8568, Japan.

SUPPLEMENTARY NOTE 1: Principle of Fresnel reflection-based columnar photonic scintillator

1.1 Basics of internal multiple reflection

The light intensity I is defined as follows:

$$\begin{aligned} I &= (1-R_2)I_0 + R_1R_2(1-R_2)I_0 + \cdots \\ &= (1-R_2)(1+R_1R_2+{R_1}^2{R_2}^2+\cdots)I_0. \end{aligned} \tag{S.1}$$

By calculating the arithmetic sequence with an initial term of 1 and common a ratio of R_1R_2, the light transmission rate T_d toward the R_2 side from the luminescence point is defined as [see Fig. S1]

$$T_\mathrm{d} = \frac{1-R_2}{1-R_1R_2}. \tag{S.2}$$

Similarly, the light transmission rate T_o toward the R_1 side from the luminescence point is

$$T_\mathrm{o} = \frac{R_1(1-R_2)}{1-R_1R_2}. \tag{S.3}$$

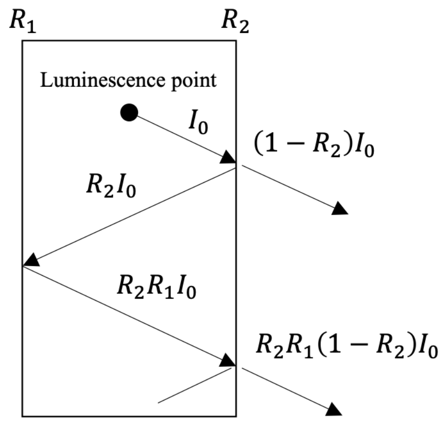

Supplementary Fig. 1 Schematic of internal reflection.

1.2 Independence of transmission power and geometrical detector size

The total power P_{t} is described as

$$P_{\mathrm{t}} = 4\pi I_0. \tag{S.4}$$

The power passing through the detector plane P_{d} [see Fig. S2] is expressed as

$$P_{\mathrm{d}} = \int d\Omega\, I_0 T(\theta,\varphi) = \int_0^{2\pi}\int_0^{\pi} I_0\, T(\theta,\varphi)\sin\theta\, d\theta d\varphi = I_0\int_0^{2\pi}\int_0^{\pi} T(\theta,\varphi)\sin\theta\, d\theta d\varphi. \tag{S.5}$$

The ranges of the zenith angle θ and the azimuth angle φ are expressed as

$$\begin{gathered} 0 \le \theta \le \frac{\pi}{2}, \\ 0 \le \varphi \le 2\pi. \end{gathered} \tag{S.6}$$

The incident angles for the XY, YZ, and ZX planes are respectively given by

$$\begin{gathered} \theta_{\mathrm{xy}} = \theta, \\ \theta_{\mathrm{yz}} = \cos^{-1}(\sin\theta\cos\varphi), \\ \theta_{\mathrm{zx}} = \cos^{-1}(\sin\theta\sin\varphi). \end{gathered} \tag{S.7}$$

Here, the light for which the incident angle on the XY plane is less than the critical angle and the critical angle or more at YZ and ZX plane, satisfy the following conditions:

$$\begin{gathered} 0 \le \theta_{\mathrm{xy}} < \theta_{\mathrm{c}}, \\ \theta_{\mathrm{c}} \le \theta_{\mathrm{yz}} \le \frac{\pi}{2}, \\ \theta_{\mathrm{c}} \le \theta_{\mathrm{zx}} \le \frac{\pi}{2}. \end{gathered} \tag{S.8}$$

These can be converted to

$$\begin{gathered} 0 \le \theta < \theta_{\mathrm{c}}, \\ 0 \le \theta < \sin^{-1}\left(\frac{\cos\theta_{\mathrm{c}}}{\cos\varphi}\right), \\ 0 \le \theta < \sin^{-1}\left(\frac{\cos\theta_{\mathrm{c}}}{\sin\varphi}\right), \end{gathered} \tag{S.9}$$

and transformed to

$$\begin{gathered} 0 \le \theta < \theta_{\mathrm{c}}, \\ \tan\theta_{\mathrm{c}} \le 1, \\ \tan\theta_{\mathrm{c}} \le 1. \end{gathered} \tag{S.10}$$

Under the condition that $\theta_c \le \pi/4$ and in the case of multiple reflection, the light transmission rate to the detector plane is expressed as

$$T(\theta) = \begin{cases} T_{\mathrm{d}}(\theta) = \frac{1-R_2(\theta)}{1-R_1(\theta)R_{2(\theta)}}, 0 \le \theta < \theta_c \\ T_{\mathrm{o}}(\theta) = \frac{R_1(\theta)(1-R_2(\theta))}{1-R_1(\theta)R_2(\theta)}, \pi-\theta_c \le \theta < \pi \end{cases}. \tag{S.11}$$

Finally, we obtain the P_{d} value as follows:

$$P_{\mathrm{d}} = \frac{P_{\mathrm{t}}}{2}\left(\int_0^{\theta_c}\sin\theta\, d\theta\frac{1-R_2(\theta)}{1-R_1(\theta)R_{2(\theta)}} + \int_{\pi-\theta_c}^{\pi}\sin\theta\, d\theta\frac{R_1(\theta)(1-R_2(\theta))}{1-R_1(\theta)R_2(\theta)}\right), \theta_c \le \pi/4. \tag{S.12}$$

As the condition of $\theta_c < \pi/4$ is satisfied, the independence condition between the light power passing through the detector plane and geometrical pixel size is established as follows:

$$n_{\mathrm{photo}} \ge \sqrt{2}n_0, \tag{S.13}$$

where n_{photo} and n_0 denote the material refractive index and refractive index of vacuum, respectively. In this scheme, the photonic scintillator can use two operation modes. One is effective under the condition $\theta_c < \pi/4$ (diffuse reflection mode). As indicated by Equation (S.12), the scale of the integration range is small owing to the small critical angle. Therefore, the internal circulating lights, shown in Fig. S3, is converted to a random angle by the top surface diffuse reflection [red arrow in Fig. S3], and this part of the light enters the detector. Meanwhile, if the critical angle is nearly equal to or less than $\pi/4$ (Fresnel reflection mode), the internal circulating light is negligible. Thus, by employing the top surface as Fresnel reflection, the detectable power is maximized based on Equation (S.12).

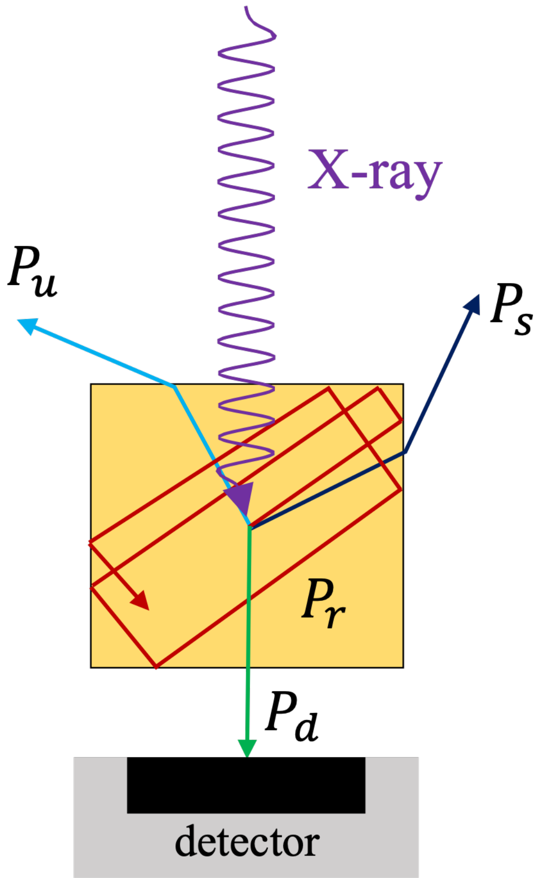

Supplementary Fig. 2 Definition of reflection power in planes.

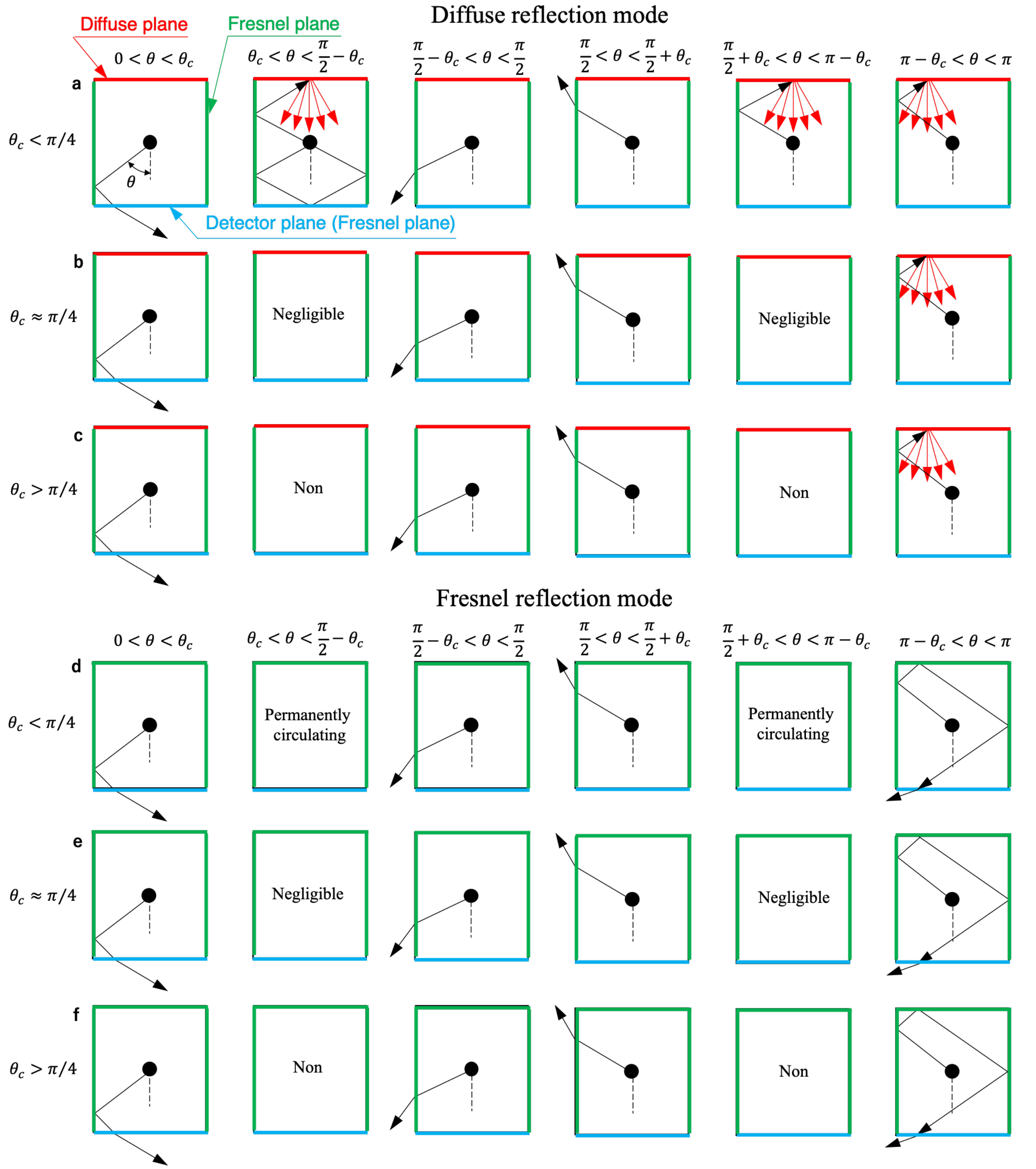

Supplementary Fig. 3 Schematic drawing of reflection patterns in a single scintillator voxel. Diffuse reflection is assumed to occur only at the top surface (red line), while Fresnel reflection is applied to all other surfaces. The diffuse reflection surface is assigned to the X-ray irradiation surface opposite the detector due to engineering constraints.

SUPPLEMENTARY NOTE 2: Simulation parameters

Supplementary Table 1 Simulation parameters for the ray tracing.

Material refractive index	1.9
Outside of material refractive index	1.0
Inside of wall refractive index	1.0
Entire material size (μm)	X: 1000, Y: 1000, Z: 800
Pixel size (μm)	200×200
Wall thickness (μm)	20
Wall height (μm)	720
Reflection definition	(top) Fresnel reflection and diffuse reflection (bottom, detector) Fresnel reflection (side) Fresnel reflection

SUPPLEMENTARY NOTE 3: Evaluation of line pair resolution without flat panel detector

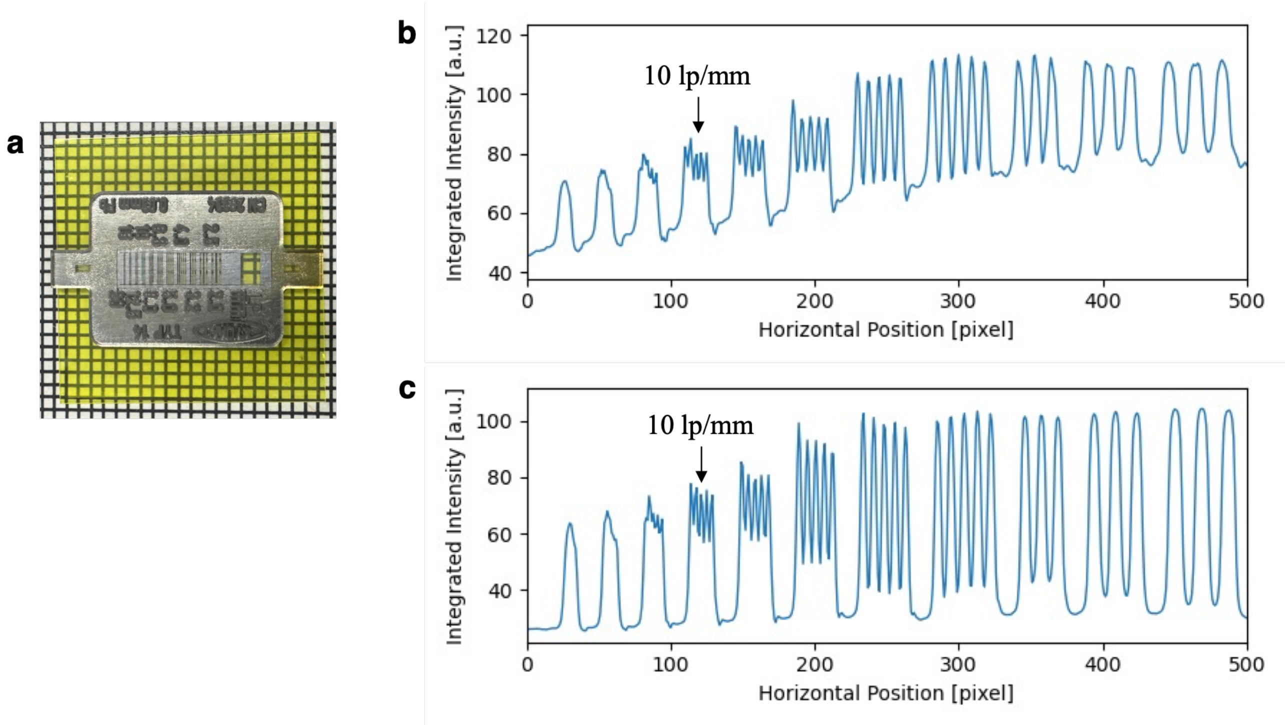

Supplementary Fig. 4 Evaluation of line-pair resolution. **a** Picture of line resolution chart for X-ray on the photonic scintillator. **b,c** Spatial line resolution comparison of **b** the photonic and **c** homogeneity GAGG scintillator. The image acquisition was 2 s and X-ray tube voltage was 50 kV.

SUPPLEMENTARY NOTE 4: Experimental setup of laser material processing

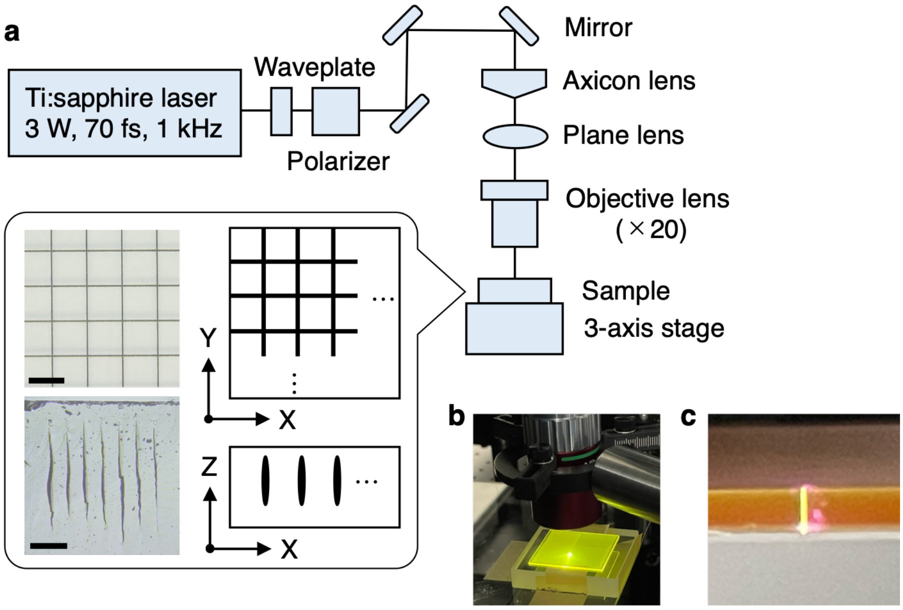

Supplementary Fig. 5 Fabrication process of the two-dimensional photonic scintillator. **a** Femtosecond laser material processing setup with Bessel beam optics and the optical micrograph of laser-treated GAGG. The scale bar corresponds to 200 µm. **b** Photograph taken during laser treatment. **c** Photograph taken during Bessel beam irradiation. The GAGG substrate is coated with an orange-colored photoresist owing to the photograph image contrast.

SUPPLEMENTARY NOTE 5: Transmission rate in GAGG:Ce with thickness of 0.8 mm.

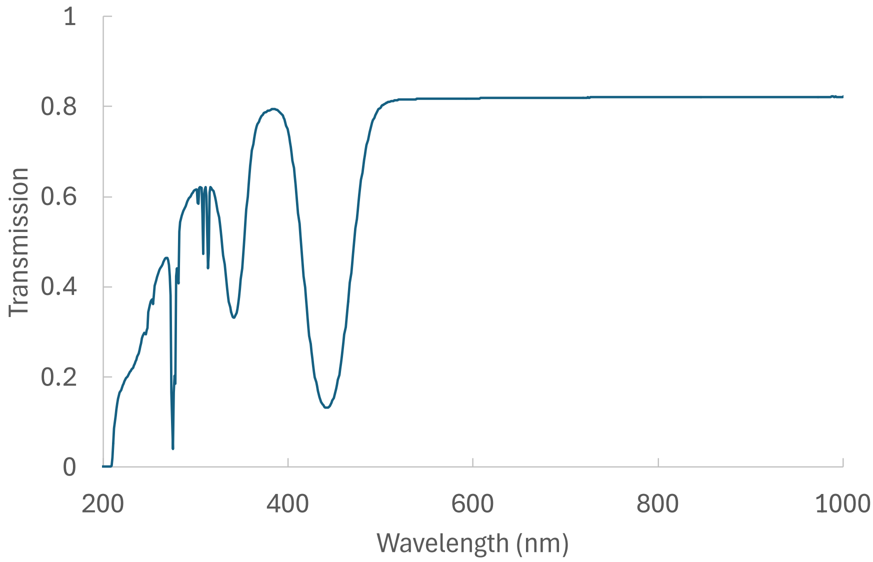

Supplementary Fig. 6 Transmission rate of GAGG:Ce (0.8 mm thickness) obtained using a spectrophotometer.